Electronic Supplementary Material (ESI) for Nanoscale Horizons.

Understanding the Noble Metal Modifying Effect on In_2O_3 Nanowires: Highly Sensitive and Selective Gas Sensors for Potential Early Screening of Multiple Disease

Wei Liu,[a]‡ Jiao Sun,[b]‡ Lin Xu,[a] Shidong Zhu,[a] Xiangyu Zhou,[a] Shuo Yang,[a] Biao Dong,[a] Xue Bai,[a] Geyu Lu,[a] Hongwei Song*[a]*

[a] State Key Laboratory of Integrated Optoelectronics, College of Electronic Science and Engineering, Jilin University, Changchun, 130012, People's Republic of China

[b] Department of Cell Biology, College of Basic Medical Sciences, Jilin University, Changchun, 130012, People's Republic of China

* E-mail: linxu@jlu.edu.cn, songhw@jlu.edu.cn

‡ These authors contributed equally to the work.

Experimental Section

Characterization.

The surface morphology of the as-prepared NWs was inspected using a JEOL JSM—7500F SEM at an accelerating voltage of 15 kV with gold sputtered on the samples. TEM and HR-TEM images were recorded on a JEM—2010 transmission electron microscope under a working voltage of 200 kV. The phase structures were characterized by XRD which were conducted on Rigaku D/max 2550 X-ray diffractomete using a mono-chromatized Cu target radiation source (λ=1.5045Å). The corresponding lattice constants were calculated by MDI Jade 5.0 software. The chemical components and bonding states of the samples were investigated by XPS using an ESCAlab250 Analytical XPL spectrometer with a monochromatic Al K-α source. The fitted peaks in XPS spectra were deconvoluted using the XPS Peak 4.1 software. The BET surface area was confirmed by the N_2 adsorption-desorption isotherms (ASAP 2420, Micromeritics) at 77 K. The gas sensing properties were measured using a WS-30 gas sensing system, which was purchased from Weisheng Instruments Company (Zhengzhou, China).

Informed Consent Statement and Collection of Breath Samples.

In this work, all participants provided informed consent for the collection of breath samples. Exhaled breath samples were collected from health volunteers at the State Key Laboratory of Integrated Optoelectronics of China. All the volunteers were asked to not eat anything after their meals for 2 h and to rinse their mouths with clean water for three times (10 min before testing). These samples were collected inside the gas collection bags (1 L) with an aluminum coating (De Lin Instrument Company, Dalian). Finally, the samples were injected into the sensing measurement system using a diaphragm pump and mixed with 2 ppm hydrogen sulfide, 1.2 ppm formaldehyde, and 1.8 ppm acetone, respectively.

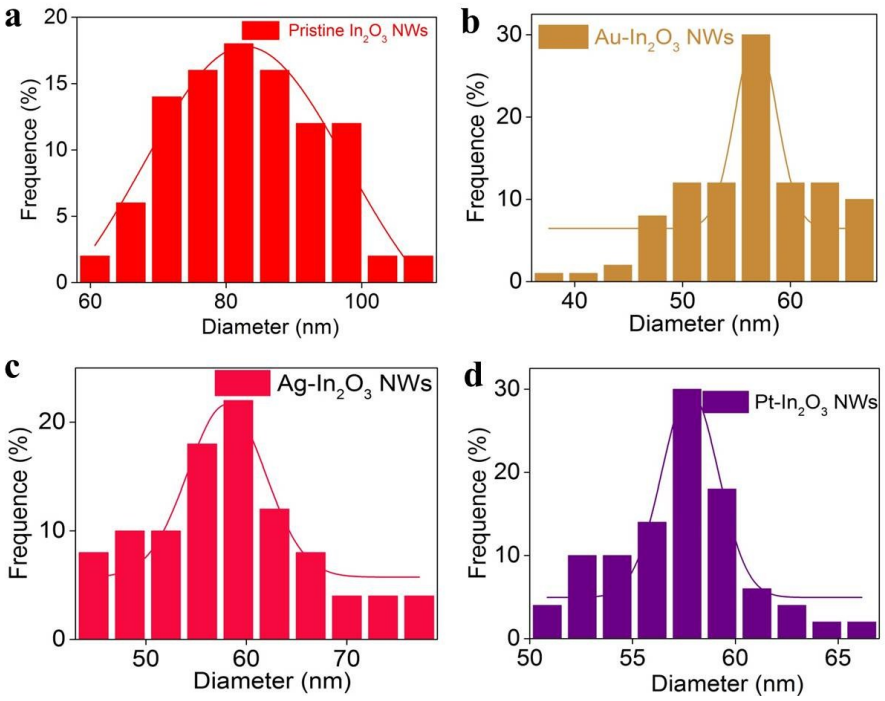

Fig. S1 The diameter distribution of (a) pristine In_2O_3 NWs (b) Au-In_2O_3 NWs, (c) Ag-In_2O_3 NWs, and (d) Pt-In_2O_3 NWs.

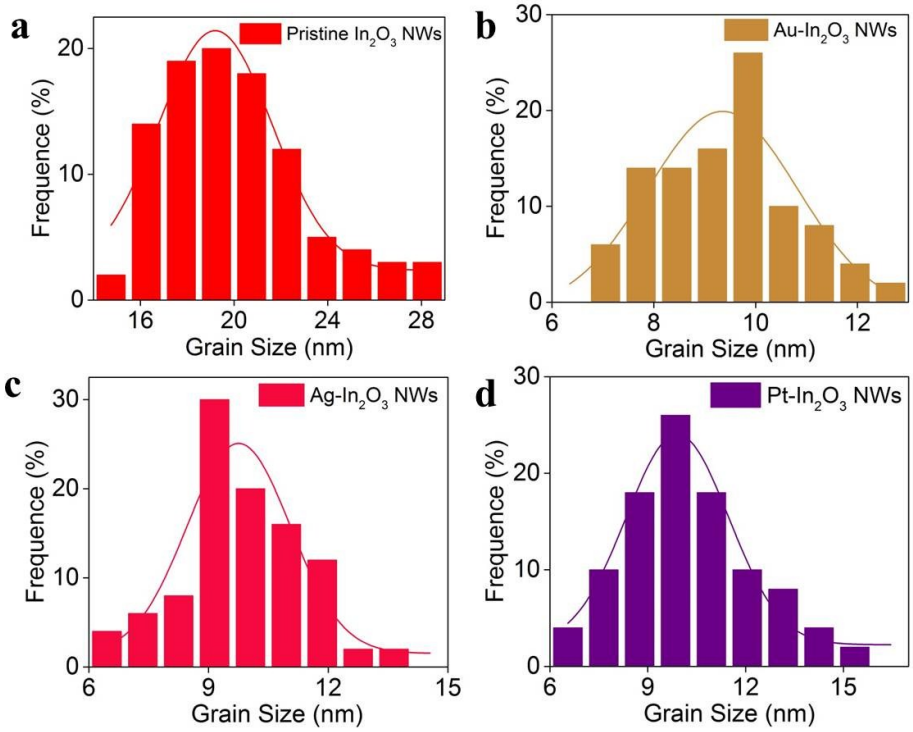

Fig. S2 The grain size distribution of (a) pristine In_2O_3 NWs (b) Au-In_2O_3 NWs, (c) Ag-In_2O_3 NWs, and (d) Pt-In_2O_3 NWs.

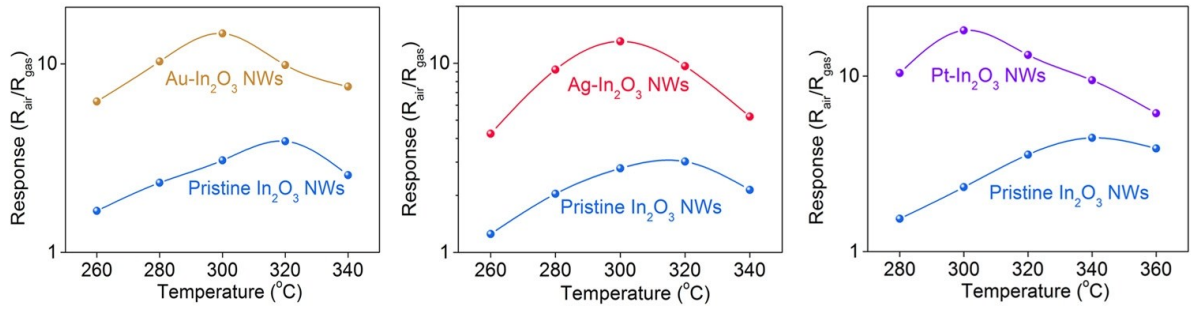

Fig. S3 The response versus working temperature to 1 ppm H_2S, formaldehyde, and acetone for Au-In_2O_3 NWs, Ag-In_2O_3 NWs, and Pt-In_2O_3 NWs, respectively.

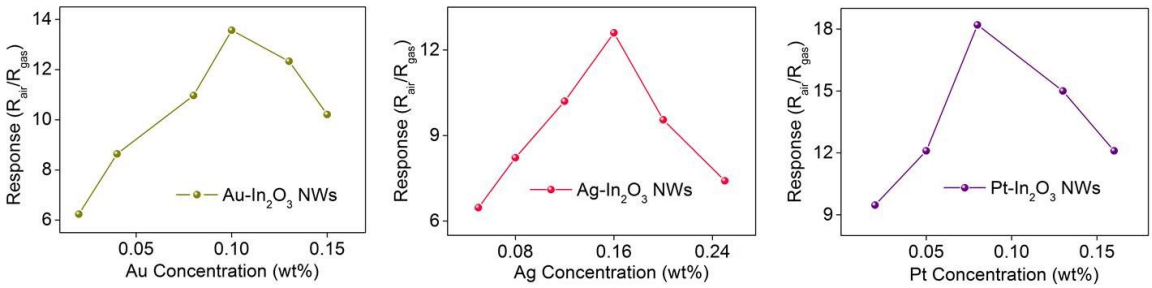

Fig. S4 Change of the concentration of NMNPs for the NMNPs modified In_2O_3 NWs sensors exposure to 1 ppm H_2S, formaldehyde, and acetone at 300°C, respectively.

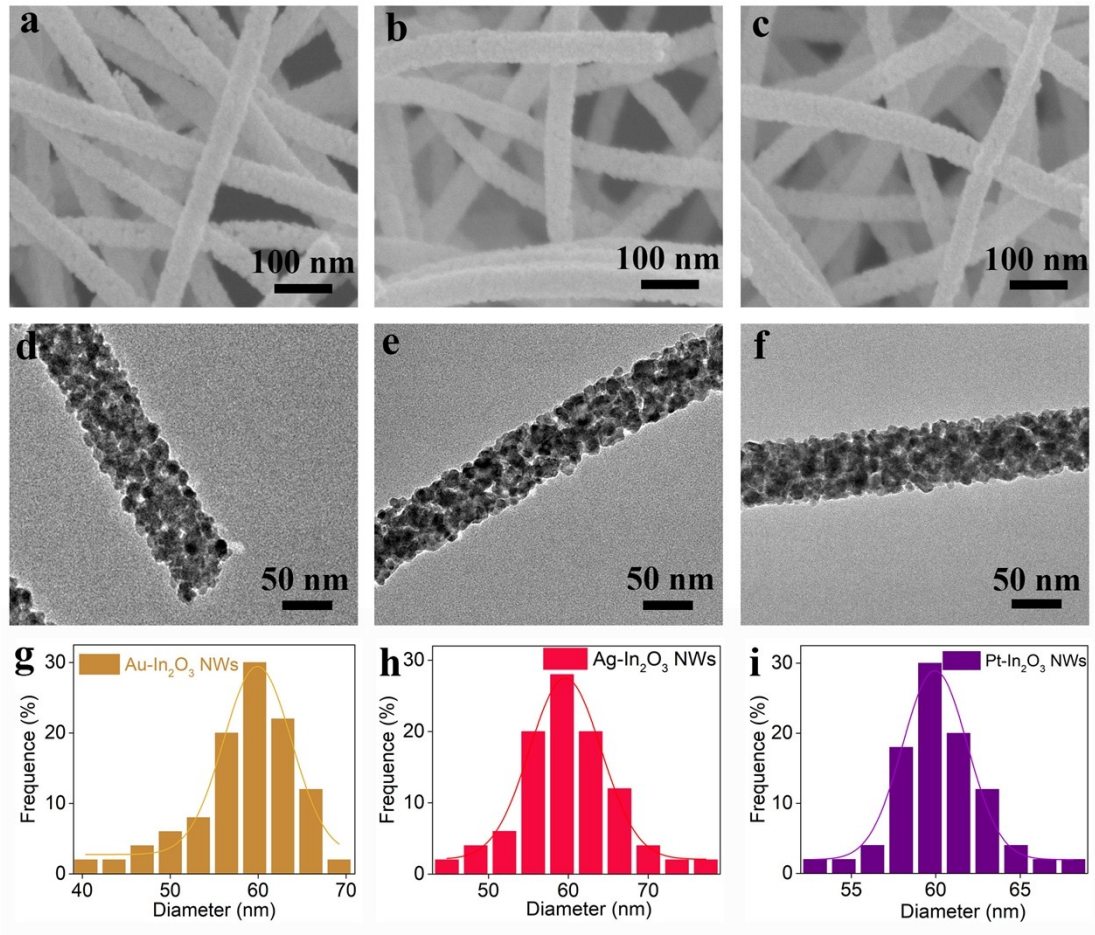

Fig. S5 Control synthesis of different NMNPs modified In_2O_3 NWs with the similar morphologies and average diameters. All the loading amount of NMNPs are fixed to be 0.08 wt.%. The SEM images of (a) Au-, (b) Ag-, and (c) Pt-In_2O_3 NWs. The TEM images of (d) Au-, (e) Ag-, and (f) Pt-In_2O_3 NWs. Diameter distribution of (g) Au-, (h) Ag-, and (i) Pt-In_2O_3 NWs.

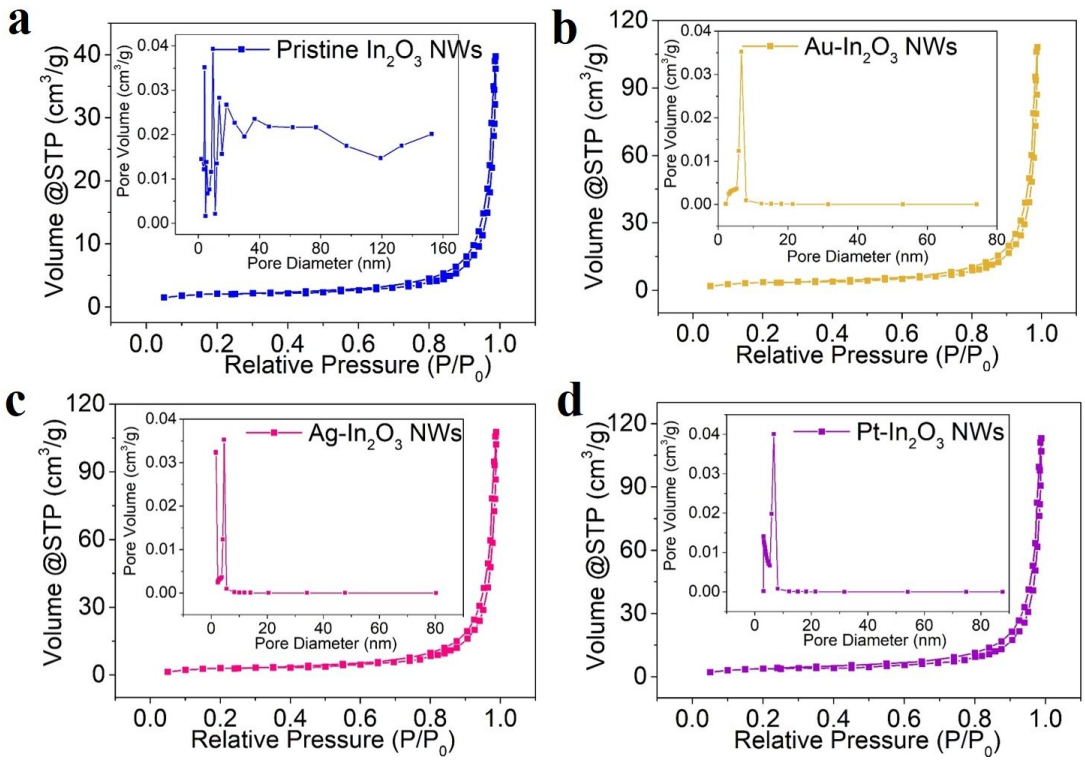

Fig. S6 The typical nitrogen adsorption–desorption isotherm and BJH pore-size distribution of (a) pristine In_2O_3 NWs, (b) Au-, (c) Ag-, and (d) Pt-In_2O_3 NWs, respectively.

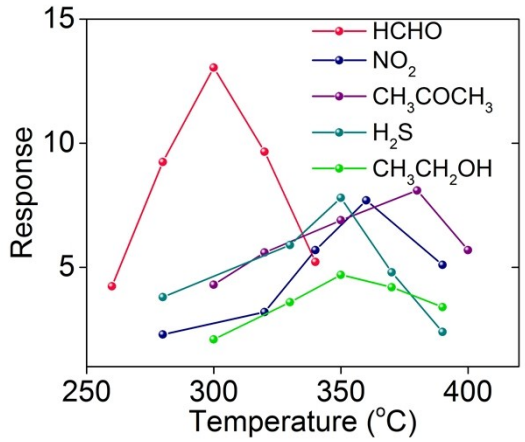

Fig. S7 The response of Ag-In_2O_3 NWs sensor versus working temperature to 1 ppm different interference gases.

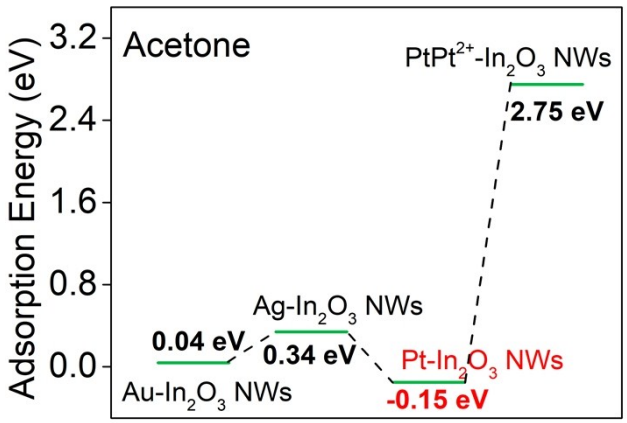

Fig. S8 The adsorption energy of Au-, Ag-, and Pt-In_2O_3 sensors for acetone.

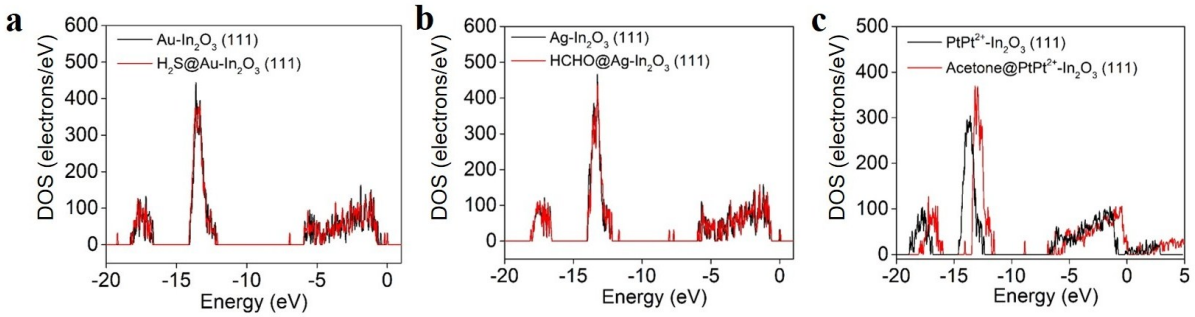

Fig. S9 The DOS of Au-, Ag-, and $PtPt^{2+}$-In_2O_3 NWs sensors before and after the adsorption of H_2S, HCHO, and acetone.

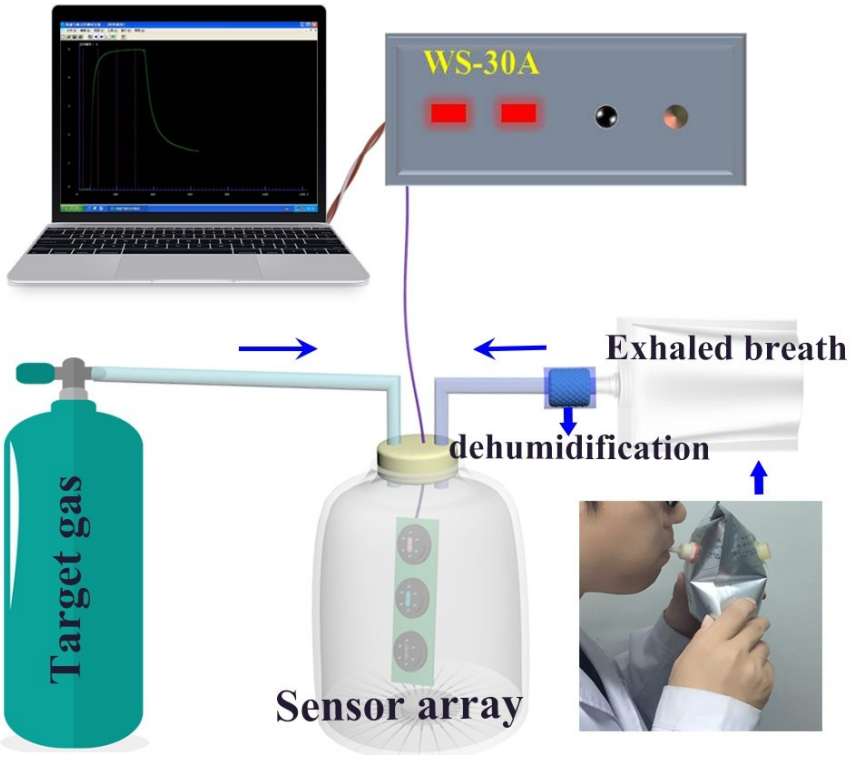

Fig. S10 Schematic illustration of the measurement system for sensing real and simulated (halitosis, breast cancer, and diabetes) breath.

Table S1. The gas-sensing performance of typical semiconductor oxide-based gas sensor arrays, and compared with that of the NMNPs modified In_2O_3 sensor in this work.

Material Systems	Gas Species	Working Temperature (°C)	Detection Range (ppm)	Real Detection Limit (ppm)	Response/ Recovery times (s)	Application Environment	Reference
MBA/Ag/$LaFeO_3$	Acetone	125	1-40	1	10/100		1
FA/Ag/$LaFeO_3$	Benzene	140	1-40	1	15/100	Indoor air	
MAA/Ag/$LaFeO_3$	Methanol	130	1-40	1	15/95		
AM/Ag/$LaFeO_3$	HCHO	125	1-40	1	10/95		
Ga_2O_3/SnO_2	Ethanol	300	10-100	10	10/56	-	2
ZnO/SnO_2	Acetone	300	10-100	10	5/10		
WO_3/SnO_2	Xylene	300	10-100	10	12/12		
Pristine SnO_2	NO_2	150	0.05-2.5	0.05	1200/2400	Exhaled	3
Pt/SnO_2	H_2	300	0.125-2.5	0.125	-/-	breath	
Pt/SnO_2	Acetone	350	0.1-5	0.1	-/-	Exhaled	4
Pd/SnO_2	Toluene	300	0.1-5	0.1	-/-	breath	
Zn/MoS_2	NO_2	25	30-100	30	20.7/38.2	Pollutants air	5
5%Zn^{2+}/MoS_2	O_3	25	0.6-5	0.6	13.5/24.3		
Pt/Rh-WO_3	Acetone	350	0.1-5	0.1	4/176	Exhaled	6
Pt/NiO-WO_3	H_2S	300	0.1-5	0.1	4.4/240	breath	
Pt/WO_3	Acetone	350	0.01-5	0.01	20.48/33.12	Exhaled	7
Pd/WO_3	Toluene	350	0.01-5	0.01	8.56/9.2	breath	
Rh/WO_3	H_2S	350	0.01-5	0.01	31.26/29.28		
Au/WO_3	H_2S	350	0.1-5	0.1	-/-	Exhaled	8
Pt/WO_3	Acetone	400	0.1-5	0.1	-/-	breath	
Pristine WO_3	H_2S	300	1-5	1	-/-	Exhaled	9
Pd/WO_3	Toluene	350	0.02-5	0.02	10.9/16.1	breath	
Mn/ZnO	Ethanol	340	5-100	5	11.4/12.4	_	10
CdO/Mn/ZnO	Acetone	240	5-100	5	10/15		
Au/In_2O_3	H_2S	300	0.05-50	0.05	35/108	Exhaled	This work
Ag/In_2O_3	HCHO	300	0.008-50	0.008	19/24	breath	
Pt/In_2O_3	Acetone	300	0.02-50	0.02	22/28		

References

1. Y. Zhang, J. Zhao, T. Du, Z. Zhu, J. Zhang and Q. Liu, *Sci. Rep.*, 2017, **7**, 1960.
2. L. Song, L. Yang, Z. Wang, D. Liu, L. Luo, X. Zhu, Y. Xi, Z. Yang, N. Han and F. Wang, *Sens. Actuators, B*, 2019, **283**, 793-801.
3. B.-H. Jang, O. Landau, S.-J. Choi, J. Shin, A. Rothschild and I.-D. Kim, *Sens. Actuators, B*, 2013, **188**, 156-168.
4. J. S. Jang, S. Yu, S. J. Choi, S. J. Kim, W. T. Koo and I. D. Kim, *Small*, 2016, **12**, 5989-5997.
5. L. Shao, Z. Wu, H. Duan and T. Shaymurat, *Sens. Actuators, B*, 2018, **258**, 937-946.
6. S. J. Kim, S. J. Choi, J. S. Jang, H. J. Cho, W. T. Koo, H. L. Tuller and I. D. Kim, *Adv. Mater.*, 2017, **29**, 1700737.
7. S.-J. Kim, S.-J. Choi, J.-S. Jang, N.-H. Kim, M. Hakim, H. L. Tuller and I.-D. Kim, *ACS nano*, 2016, **10**, 5891-5899.
8. S. J. Choi, S. J. Kim, H. J. Cho, J. S. Jang, Y. M. Lin, H. L. Tuller, G. C. Rutledge and I. D. Kim, *Small*, 2016, **12**, 911-920.
9. N.-H. Kim, S.-J. Choi, D.-J. Yang, J. Bae, J. Park and I.-D. Kim, *Sens. Actuators, B*, 2014, **193**, 574-581.
10. J. Wang, J. Yang, N. Han, X. Zhou, S. Gong, J. Yang, P. Hu and Y. Chen, *Mater. Des.*, 2017, **121**, 69-76.